Chapter 1

Introduction

1. Overview

From supporting our everyday lives to promoting cutting-edge technological advancements, fossil fuels have played a very important role for our civilization. As the finite amount of fossil reserves are being depleted at a rate that will not sustain the continuing growing human population, the need for affordable alternative energy sources has become more prominent. Renewable energy sources, like wind, hydro, and solar powers, are abundant and can be harnessed and utilized without further polluting our green planet. However, the well-established infrastructure for the extraction and distribution of fossil fuel-derived power has allowed the cost to remain relatively low, making more expensive solar energy less attractive. As people start to recognize our unsustainable practice of energy consumption, many may soon start to incorporate solar energy as part of their primary power source. For the prevalent utilization of solar energy to become a reality in a near future, scientists have to develop more efficient solar energy conversion devices while lowering the costs at the same time. Understanding the basic concepts of semiconductor junctions is the first step towards this goal.

The plants have evolved to make extensive use of solar energy in photosynthesis to convert sun light directly into stored fuels. Typical photosynthetic process, however, convert only 3–5% of the total incident solar power into fuel storage,[1] yet is sufficient to sustain life on Earth. On the other hand, the conversion of photon energy into electrical energy has been realized in photovoltaic devices consisting of two different solids connected at an abrupt junction which has the ability to direct electrical current flow in one direction through the external circuit.[2] These solid-state devices are currently being used for some applications; however, the required use of single crystals and the formation of abrupt junction make the cost of energy so produced too high to compete with that generated by burning fossil fuels. Although modern devices are quite efficient and

durable,[3] with such small economic value, the wide implementation of photovoltaic devices is proved to be difficult. A less-expansive solar energy conversion can be achieved by photoelectrochemical cells, which involve the use of semiconductor to adsorb incident light and the electrochemical process at semiconductor/liquid junction to allow energy conversion. The photoelectrochemical cells can be constructed to produce electricity or to store chemical fuels, and the efficiencies are generally between those of photovoltaics and photosynthesis.[1]

The basic challenge in developing practical photoelectrochemical solar energy conversion devices is the trade-off between the semiconductor stability and conversion efficiency.[1] Semiconductors with relatively high bandgap energies, such as titanium dioxide (TiO_2), absorb high-energy photons but only a small portion of the solar spectrum. TiO_2 is stable in aqueous solutions, but suffers a poor solar-conversion efficiency of about 1%. Materials made of germanium have very small bandgaps that can absorb a large fraction of the solar spectrum; unfortunately, a significant amount of absorbed energy is wasted as heat when the highly excited electrons readily relax to the energy of the conduction band edge. Semiconductors with moderate bandgaps, such as silicon (Si), gallium arsenide (GaAs), and indium phosphide (InP), are unstable in aqueous solutions, but prove to be the most efficient due to a well-overlapped bandgap energies with terrestrial solar spectrum.

The contacts between moderate bandgap semiconductors and aqueous electrolytes frequently result in photocorrosion or photopassivation of the electrode surfaces, which significantly limits the device lifetimes. One solution to this problem is the addition of a redox reagent that can compete kinetically with undesirable surface reactions. The difficulty involved is the extraordinary requirement of an extremely efficient redox species with very fast kinetics; otherwise the photocorrosion or photopassivation processes cannot be completely prevented. Another approach would be replacing the aqueous solution phase with a non-aqueous electrolyte system. Although the

combination is often toxic and not yet suitable for the commercial use, the semiconductor/non-aqueous liquid contacts are ideal for scientific investigation due to the constructional simplicity. Understanding of photoelectrochemical processes at these junctions is viable for future improvements of solar energy conversion devices.

This thesis includes investigations of charge-carrier dynamics at semiconductor junctions through the effects of surface modifications. A brief introduction to the fundamental theory of semiconductor heterojunctions and charge-carrier recombination process is included in this chapter. Chapter 2 presents both electrochemical and surface investigations of n-GaAs/CH$_3$CN interfaces. It also addresses the very importance of understanding the charge-carrier recombination mechanism in correctly assessing the electron-transfer processes across a semiconductor/liquid junctions. Chapter 3 describes an attempt to fabricate metal-insulator-semiconductor (MIS) diodes for improved electrical properties of a metal-semiconductor junction by surface modification of Si. Although problems exist that complicated the junction formation, some preliminary results offered valuable insights and hopes. Chapter 4 turns the focus back into the semiconductor surface chemistry and describes a surface modification procedure capable of producing stable Si surfaces that prevented the increase of surface defect density when exposed to air. The work included can be of importance for several technologies, and possible applications may not be limited to photovoltaics or photoelectrochemical cells.

2. Charge-Transfer Equilibration at Semiconductor Heterojunctions[1,4]

When a semiconductor comes into contact with a liquid or a metal phase, the difference in the electrochemical potential of the semiconductor and the contacting phase results in charge equilibration at the heterojunction. Since works present in this thesis involve n-GaAs and n-Si, the ideal junction between an n-type semiconductor and a contacting phase with a more positive electrochemical potential is described. The electrochemical potential of a freestanding semiconductor is set by the position of its Fermi level ($\mathbf{E}_F$), which is the energy level where the probability of finding an electron is one-half. When a solution containing a redox couple A/A⁻ (A is an electroactive acceptor and A⁻ is a donor) is the contacting phase, the electrochemical potential of the contacting phase ($\mathbf{E}_{F,c}$) is $\mathbf{E}(A/A^-)$ and is given by the Nernst equation:

$$\mathbf{E}(A / A^-) = \mathbf{E}^{\circ\prime}(A / A^-) + (kT)\ln([A]/[A^-]) \qquad (1.1)$$

where $\mathbf{E}°´(A/A^-)$ is the electrochemical potential of the redox couple A/A⁻ under standard-state conditions, k is the Boltzmann's constant, and T is the absolute temperature. When the contacting phase is a metal the $\mathbf{E}_{F,c}$ is $\mathbf{E}_{F,m}$. Since it is difficult to experimentally determine the value of $\mathbf{E}_{F,m}$, work function of the metal (φ_m) is often used instead of $\mathbf{E}_{F,m}$.

When two phases are brought into contact, electrons flow from the phase with more negative initial electrochemical potential to the other, in this case from the semiconductor to the contacting phase, until the electrochemical potentials of both phases are in equilibrium. As the result of this charge-transfer process, both the semiconductor and the contacting phase lose their original charge neutrality. Excess positive charges are produced in the semiconductor while an excess of negative charges appears in the contacting phase. Since the number of available states per unit energy in the solution,

even with dilute concentration of redox species, or the metal far exceeds the number in a semiconductor, the accepted negative charges do not change the position of the $\mathbf{E}_{F,c}$. On the other hand, the Fermi level of the semiconductor becomes more positive, and the equilibrium position of the Fermi level for both phases is essentially equal to the initial value of the $\mathbf{E}_{F,c}$.

During the equilibration process, electrons that are the most easily ionized are removed first. This means that the charges are removed from dopant atoms before Si atoms are ionized. Since a certain number of electrons are needed from the semiconductor in order to reach the charge-transfer equilibrium, usually more than an atomic layer of dopant atoms are ionized. The distance into the semiconductor from the interface that is required for removal of charges from all the dopant atoms within this region is called the depletion width (W), and the region is called depletion region. A more positive initial $\mathbf{E}_{F,c}$ or a more negative initial $\mathbf{E}_F$ requires more layers of dopant atoms to be ionized, hence a larger W. The charge-transfer equilibration causes electric fields and electric potential gradients to rise in both phases, and the presence of this electric field at the interface is essential for the effective charge separation at semiconductor/liquid junction to separate charge effectively. A band bending diagram is used to depict the potential energy vs. distance relationship for a semiconductor/liquid junction (Figure 1.1) and for a semiconductor/metal junction (Figure 1.2). The electric potential energy levels of both conduction band ($\mathbf{E}_{cb}$) and valence band ($\mathbf{E}_{vb}$) drop within the depletion width as moving away from the interface and into the bulk of semiconductor. A barrier height (ϕ_b) is thus formed at the interface, and the barrier height energy ($q\phi_b$) is defined as the differences between the equilibrium Fermi level and the energy of the conduction band edge. In the case of semiconductor/metal junction, the ϕ_b can be calculated using thermodynamic model:[5,6]

$$\phi_b = (\varphi_m - \chi_s) / q \qquad\qquad (1.2)$$

where φ_m is the work function of the metal (in eV) and χ_x is the electron affinity of the semiconductor.

Figure 1.1

A band bending diagram for an ideal n-type semiconductor/liquid junction before equilibrium (a) and at equilibrium (b). (a) Before charge-transfer equilibration occurs, the energy levels of the conduction and the valence bands of the semiconductor are the same everywhere from the surface to the bulk. When a semiconductor with a more negative Fermi level ($\mathbf{E}_F$) is brought into contact with a solution with a redox potential $\mathbf{E}(A/A^-)$, electrons flow from the semiconductor to the solution phase. (b) After charge-transfer equilibration has occurred, a depletion layer of a width W formed in the semiconductor, and the contact potential drops primarily across this region. The Fermi level is the same across the junction at all points. The parameter qV_n is defined as the difference between $\mathbf{E}_F$ and $\mathbf{E}_{cb}$ in the bulk, V_{bi} is the built-in voltage of the junction, and the barrier height (ϕ_b) is defined as $\phi_b = V_{bi} + V_n$, and $q\phi_b$ is the difference between $\mathbf{E}_{cb}$ at the interface and $\mathbf{E}(A/A^-)$ of the solution.

Energy (eV)

(−)

(+)

$\mathbf{E}_{cb}$

$\mathbf{E}_F$

qV_n

$\mathbf{E}_{vb}$

e^-

$\mathbf{E}(A/A^-)$

Semiconductor

Solution

x=0

(a)

$\mathbf{E}_{cb}$

qV_{bi}

qV_n

$\mathbf{E}_F$

$\mathbf{E}_{vb}$

$q\phi_b$

W

$\mathbf{E}(A/A^-)$

Semiconductor

Solution

x=W

x=0

(b)
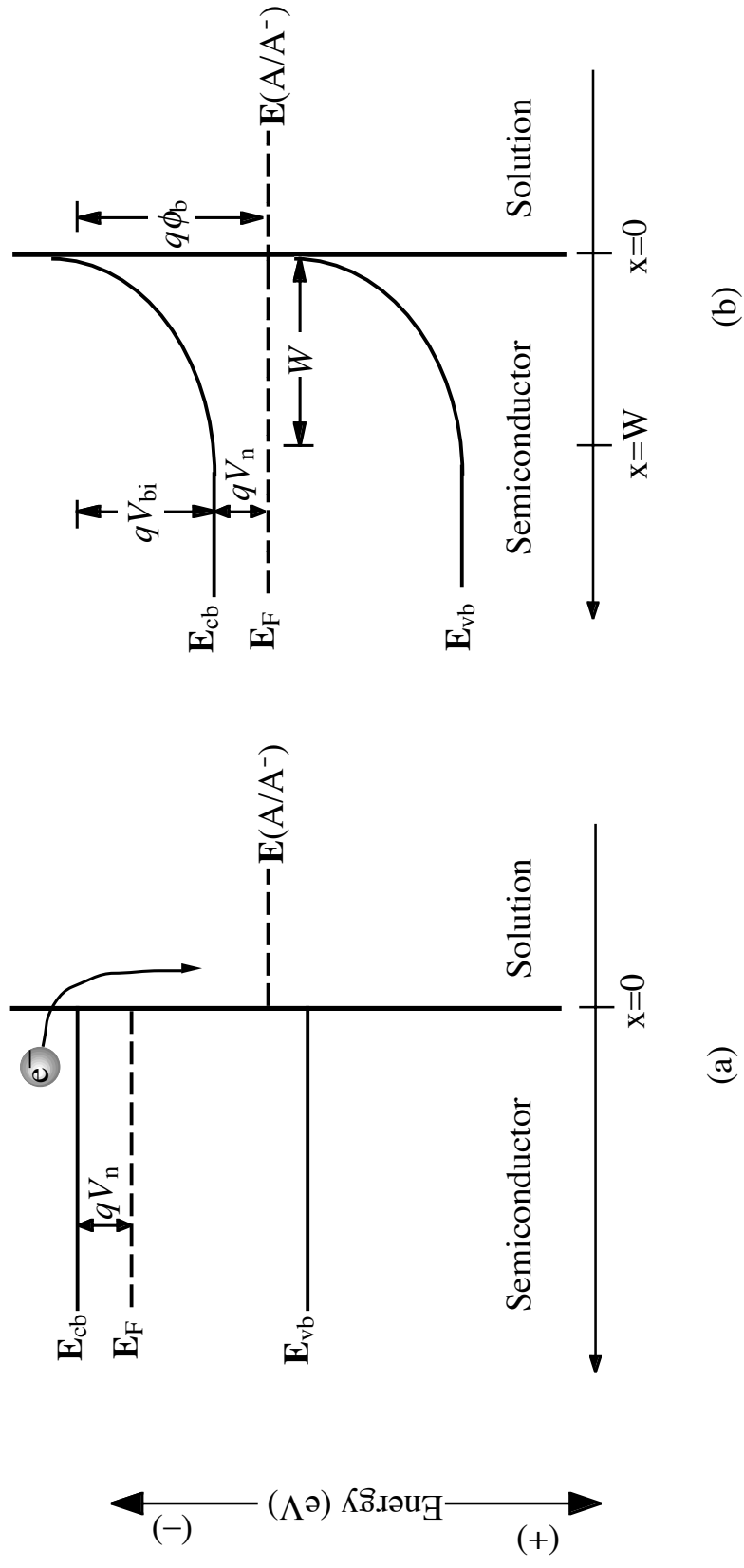
Figure 1.2

A band bending diagram for an ideal n-type semiconductor/metal junction before

equilibrium (a) and at equilibrium (b). (a) Before charge-transfer equilibration occurs,

the energy levels of the conduction a valence bands of the semiconductor are the same

everywhere from the surface to the bulk. When a semiconductor with a more negative

Fermi level ($\mathbf{E}_F$) is brought into contact with a metal with a Fermi level ($\mathbf{E}_{F,m}$), electrons

flow from the semiconductor to the metal phase. (b) After charge-transfer equilibration

has occurred, a depletion layer of a width W formed in the semiconductor and the contact

potential drops primarily across this region. The Fermi level is the same across the

junction at all points. The parameter qV_n is defined as the difference between $\mathbf{E}_F$ and $\mathbf{E}_{cb}$

in the bulk, V_{bi} is the built-in voltage of the junction, and the barrier height (ϕ_b) is defined

as $\phi_b = V_{bi} + V_n$, and is the difference between the metal work function φ_m and the electron

affinity χ_s of the semiconductor.

(a)

(b)

Energy (eV)

(−) (+)

E_{vacuum}

χ_s

E_{cb}
E_F

E_{vb}

φ_m

$E_{F,m}$

e^-

Metal

Semiconductor

x=0

E_{vacuum}

χ_s

qV_{bi}

E_{cb}
E_F

E_{vb}

φ_m

$q\phi_b$

$E_{F,m}$

W

Metal

Semiconductor

x=0
x=W
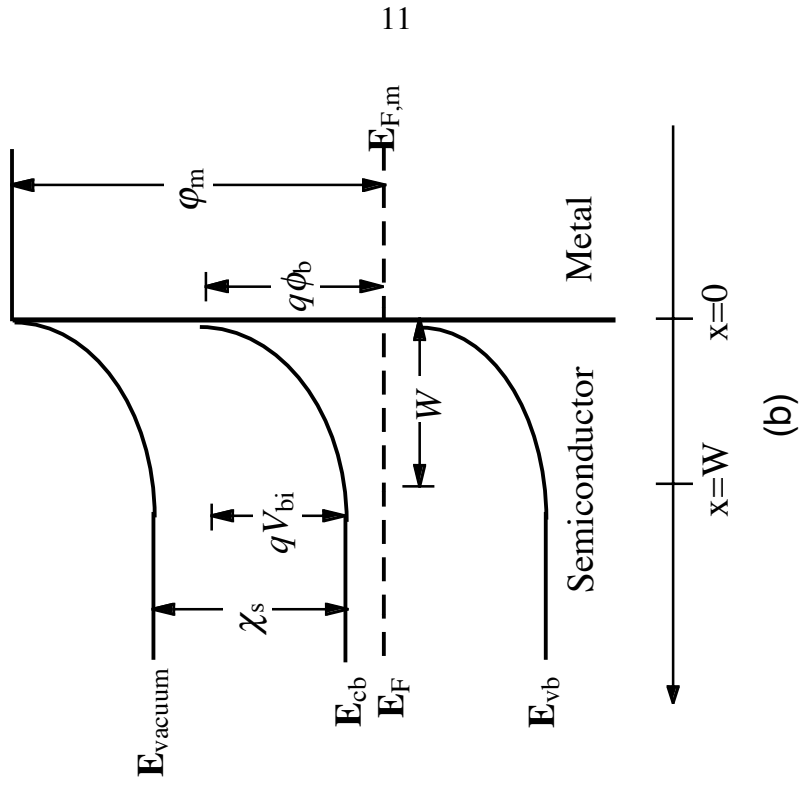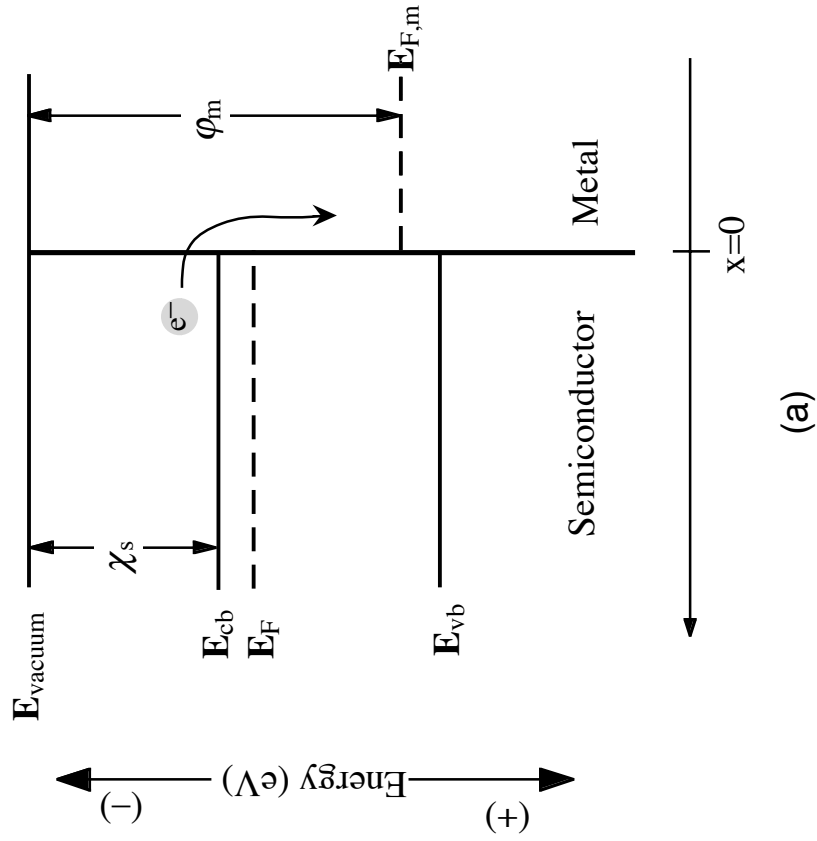
3. Current–Voltage Properties of a Semiconductor Diode

When a semiconducting material is illuminated with photons of sufficient energy ($\geq$ bandgap energy, E_g), electrons are excited from valence band orbitals to the conduction band and leave behind positively charged sites (commonly referred to as "holes"). In the absence of an electric field, these photoexcited electrons quickly relax to their ground states and recombine with the holes. With the presence of an electric field formed at the semiconductor heterojunction, photogenerated carriers can be separated since electrons have a tendency to move away from the more negative interface while holes move towards it. The photogenerated electrons can then be collected at the ohmic back contact and directed through the external circuit to do useful work. The separation of charge carriers at semiconductor/liquid and semiconductor/metal junctions is the basis of solar energy conversion by photoelectrochemical cells and photovoltaics.

The flow of electrons through the external circuit due to photoexcitation is measured as the photocurrent (J_{ph}). The current can also flow in the opposite direction of the J_{ph} due to recombination of electron-hole pairs, and this unfavorable current is called reserve saturation current or recombination current (J_0). The discussion of charge-carrier recombination mechanisms is also in order. The total current (J) flowing across an n-type semiconductor heterojunction is described by the diode equation:[3,7]

$$J = J_{ph} - J_0 \left[\exp\left(\frac{-qV}{\gamma kT} \right) - 1 \right] \tag{1.3}$$

where V is the applied voltage and γ is the diode quality factor. The anodic current is assigned positive values and the diode forward bias is negative on the electrochemical scale. The voltage developed by the photoelectrochemical cell under illumination, the open-circuit voltage (V_{oc}), is the voltage measured at $J = 0$, and is a measure of the

maximum Gibbs free energy available from the cell. For $J_{ph} \gg J_0$, equation 1.3 can be rearranged to yield

$$V_{oc} = \frac{\gamma kT}{q} \ln\left(\frac{J_{ph}}{J_0}\right) \qquad (1.4)$$

Measurements of V_{oc} and J_{ph} at several illumination intensities, combined with the use of equation 1.4, can allow the extraction of J_0. Since this measurement is performed at no net current flow, it can eliminate the problems that can distort the J–V properties of many semiconductor/liquid junctions. These potential problems include the presence of a large series resistance at high current flow and a nonlinear voltage drop due to mass transport limit of the redox species.[7-9]

4. Charge-Carrier Recombination Mechanisms[10]

Once the electron-hole pairs are generated in the semiconductor by photoexcitation, electrons and holes can find ways to recombine before being harnessed to do useful work. Generally there are five types of recombination mechanisms that can contribute to the recombination current (J_0). Depending on the location of recombination relative to the junction, the recombination pathways are grouped into either majority carrier processes or minority carrier processes. Figure 1.3 depicts several pathways that the recombination processes can occur at the semiconductor/liquid junction. All possible recombination mechanisms usually occur simultaneously for a given sample, and the total recombination current is the sum of the individual recombination currents:

$$J_0 = J_{et} + J_{tun} + J_{ss} + J_{dr} + J_{br} \qquad (1.5)$$

where subscript "et" is the recombination due to interfacial electron transfer when the contacting phase is a liquid and is replaced by "th", the thermionic emission, when the contacting phase is a metal, subscript "tun" is the recombination due to electron tunneling, subscript "ss" is the surface-state recombination, subscript "dr" is the depletion-region recombination, and subscript "br" is the bulk-region recombination. Depending on the semiconductor dopant density (N_d), barrier height, the density of surface traps located within the bandgap, and the applied bias (V), one pathway usually dominates the recombination event and therefore J_0. These recombination processes will be discussed briefly in the next two sections.

When electrons are injected into the contacting phase and recombine with holes outside of the semiconductor, it is categorized as a majority carrier recombination. Two pathways involving this process are interfacial electron transfer, or thermionic emission, and tunneling through the surface potential barrier. If the surface barrier is large or wide,

electron injection into the contacting phase might be more difficult. In this case, the rate of hole injection into the semiconductor dominates the carrier transport across the interface, and the injected holes travel through the semiconductor and can recombine with electrons via one of the three pathways: surface-state recombination, depletion-region recombination, and bulk-region recombination.
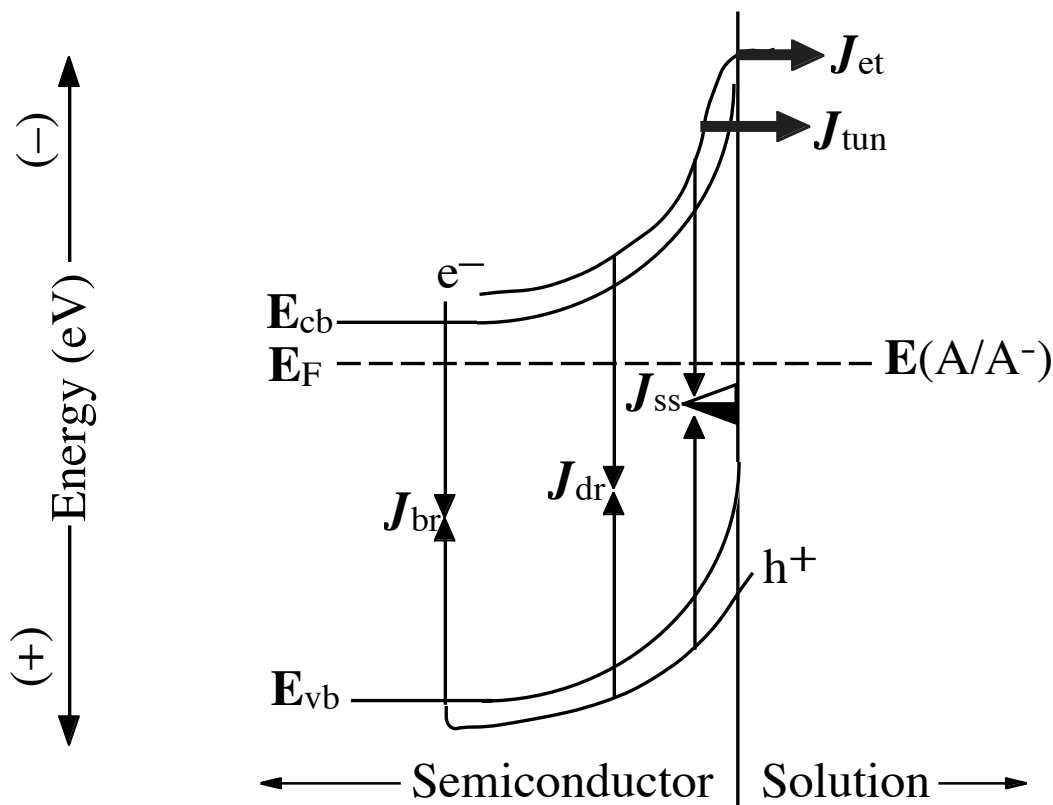
Figure 1.3

Various types of recombination pathways for an *n*-type semiconductor/liquid junction. The J_{et} is the current caused by electron transfer over the potential barrier from the semiconductor to the redox acceptors in the solution. The J_{tun} describes the majority carrier tunneling current through the potential barrier. Recombination due to the surface states near the interface results in J_{ss}, while recombination in the depletion and bulk regions produces J_{dr} and J_{br}, respectively. Both J_{et} and J_{tun} are currents requiring injection of majority carriers from the semiconductor, hence majority carrier recombination currents. On the other hand, J_{ss}, J_{dr}, and J_{br} are currents due to minority carrier recombination process, since holes are injected into the semiconductor for the recombination to occur.

4.1.   Interfacial Electron Transfer/Thermionic Emission

At semiconductor/metal junctions (Schottky junctions), the interfacial electron transfer over the top of the surface barrier is called thermionic emission. Since the metal has a very high density of unoccupied levels, every electron that reaches the top of the surface barrier is assumed to be captured by the metal phase.[7,9] The relationship between J_0 and ϕ_b can be described by the thermionic emission theory:[11]

$$J_0 = A^{**}T^2 \exp\left(\frac{-q\phi_b}{kT}\right) \qquad (1.6)$$

where A^{**} is the modified Richardson constant, which is the probability of an electron being injected into the metal once it reaches the interface. Since ϕ_b is not a function of N_d, the thermionic emission current is independent of the dopant density of semiconductor. When the thermionic emission is the dominant recombination mechanism, the experimentally determined γ is 1, and the activation energy is $q\phi_b$.

At semiconductor/liquid junctions, the interfacial electron-transfer event is governed by both the concentration of electrons at the semiconductor surface (n_s) and the concentration of acceptor species in solution ([A]). The recombination current can be expressed as:[12,13]

$$J_0 = qk_{et}n_s[A] \qquad (1.7)$$

where k_{et} is the rate constant for electron transfer from the semiconductor to the redox acceptor in solution.

4.2.   Electron Tunneling

The electron tunneling rate can be calculated with quantum theory by modeling the potential barrier as triangular. The probability of tunneling through the base of the barrier is

$$T_{tun} = \exp\{-8\pi W[2qm_e^*(|V_{bi}|+V)]^{1/3}/3h \tag{1.8}$$

where m_e^* is the effective mass of an electron, V_{bi} is the difference between the conduction band edge at the surface and in the bulk, and h is the Planck's constant. The total current can be described as

$$J = qv_{th}T_{tun}(\mathbf{E})dn(\mathbf{E}) \tag{1.9}$$

The rate of electron tunneling through the potential barrier usually only dominates the recombination rate when the semiconductor is highly doped. When the dopant density is high, the relatively small W results in a thin barrier, which allows electrons to cross into the contacting phase. The recombination current depends on dopant density and is a complicated function of V, T, and N_d (affects V_{bi}). If the recombination due to electron tunneling is the dominant mechanism, the experimentally determined γ is greater than 1.

4.3. Surface-State Recombination

Nonradiative recombination mediated by energy levels within the bandgap can be described by Shockley-Read-Hall (SRH) statistics.[14,15] The rate of surface-state recombination can be derived by evaluating the microscopic balance between electrons and holes capture and emission processes by recombination centers at the semiconductor surface.

Assuming a given number density of recombination centers at surface ($N_{r,s}$, cm^{-2}) exist at an energy within the bandgap $\mathbf{E}_{r,s}$ (Figure 1.4). The net rate of electron occupying these recombination centers is equal to the capture rate of electrons in conduction band minus the thermal emission rate of electrons back to the conduction band:

$$\frac{d(N_{r,s}f_{r,s})}{dt} = n_s k_{n,s} N_{r,s}(1-f_{r,s}) - k'_{n,s} N_{r,s} f_{r,s} \tag{1.10}$$

and the net rate of holes in valence band occupying these recombination centers is

$$\frac{d[N_{r,s}(1-f_{r,s})]}{dt} = p_s k_{p,s} N_{r,s} f_{r,s} - k'_{p,s} N_{r,s}(1-f_{r,s}) \tag{1.11}$$

where $f_{r,s}$ is the fraction of occupied recombination centers, n_s is the number of electrons in the conduction band, p_s is the number of holes in the valence band, $k_{n,s}$ and $k_{p,s}$ is the capture coefficient of electrons and holes by the recombination centers, and $k'_{n,s}$ and $k'_{p,s}$ is the emission coefficient of electrons and holes from the filled recombination centers. Let $n_{1,s}$ and $p_{1,s}$ be the surface electron and hole concentrations when the Fermi level is located at $\mathbf{E}_{r,s}$, $k_{n,s}$ and $k_{p,s}$ can be related to $k'_{n,s}$ and $k'_{p,s}$, respectively, using the principle of detailed balance at steady state, which tells us that each process is in equilibrium by itself and also with other processes:

$$k'_{n,s} = k_{n,s}N_c \exp[(\mathbf{E}_{r,s} - \mathbf{E}_{c,s})/kT] = k_{n,s}n_{1,s} \qquad (1.12)$$

$$k'_{p,s} = k_{p,s}N_v \exp[(\mathbf{E}_{r,s} - \mathbf{E}_{v,s})/kT] = k_{p,s}p_{1,s} \qquad (1.13)$$

N_c and N_v are the density of electronic states in the conduction band and valence band, and $\mathbf{E}_{c,s}$ and $\mathbf{E}_{v,s}$ are the energy of the conduction and valence band edges at the surface, respectively.

Under the steady-state conditions, the occupancy density of the states is constant, and the recombination rate (U_s) is equal to $d(N_{r,s}f_{r,s})/dt = d[N_{r,s}(1\text{-}f_{r,s})]/dt$. The $f_{r,s}$ can be solved by setting equations 1.10 and 1.11 equal to each other. Substituting the expression for $f_{r,s}$ back into either equation and realizing $n_{1,s}p_{1,s} = n_i^2$ (n_i is the intrinsic carrier concentration) yields

$$U_s = N_{r,s} \frac{k_{n,s}k_{p,s}(n_s p_s - n_i^2)}{k_{n,s}(n_s + n_{1,s}) + k_{p,s}(p_s + p_{1,s})} \qquad (1.14)$$

Equation 1.14 represent sthe net rate of surface-state recombination for recombination centers located at a single energy level $\mathbf{E}_{r,s}$, and the total surface-state recombination current can be obtained by integrating U_s over all possible recombination center energies. Surface recombination velocity (S) represents the pseudo-first-order rate constant for surface-state recombination of minority carrier and is commonly used to characterize the surface property of semiconductors. During photoexcitation, the surface carrier concentrations can be described as the sum of equilibrium and injected carrier concentrations ($n_s = n_{0,s} + \Delta n_s$ and $p_s = p_{0,s} + \Delta p_s$). Substituting these terms and $U_s \equiv S\Delta p_s$ into equation 1.14 results in the following expression, taking into account that $n_{0,s}p_{0,s} = n_i^2$:

$$S = N_{r,s} \frac{k_{n,s}k_{p,s}[n_{0,s} + (p_{0,s}\Delta n_s / \Delta p_s) + \Delta n_s]}{k_{n,s}(n_{0,s} + \Delta n_s + n_{1,s}) + k_{p,s}(p_{0,s} + \Delta p_s + p_{1,s})} \qquad (1.15)$$

Since S (has units of velocity, cm s^{-1}) is a function of electron and hole concentrations, the parameter depends on variables such as illumination level, applied potential, and temperature. At high level injection, concentrations of photogenerated carriers Δn_s and Δp_s are much greater than $n_{0,s}$ and $p_{0,s}$, respectively, and $\Delta n_s = \Delta p_s$. Equation 1.13 can be rewritten as:

$$S = N_{r,s} \frac{k_{n,s} k_{p,s}}{k_{n,s} + k_{p,s}} \tag{1.16}$$

At low level injection, $\Delta n_s = \Delta p_s$, $\Delta p_s \gg p_{0,s}$, and $\Delta n_s \ll n_{0,s}$; equation 1.13 can then be simplified:

$$S = N_{r,s} k_{p,s} = 1 / \tau_{p,s} \tag{1.17}$$

where $\tau_{p,s}$ is defined as minority carrier lifetime at the surface. When S is measured under either of these conditions, S is independent of carrier concentrations and allows for the extraction of surface recombination trap density without the effect of perturbation. At high level injection the slowest of either electron or hole capture dominates the S, while it is controlled only by the hole capture at low level injection. The surface-state recombination current can be expressed in a way similar to a diode equation by factoring out the injected carrier concentration Δp_s:

$$J = qU = qSp_{0,s}[\exp(-qV / kT) - 1] \tag{1.18}$$

From equation 1.18, γ is predicted to be 1 for surface-state recombination, although it can be higher than 1 under the low level injection condition.
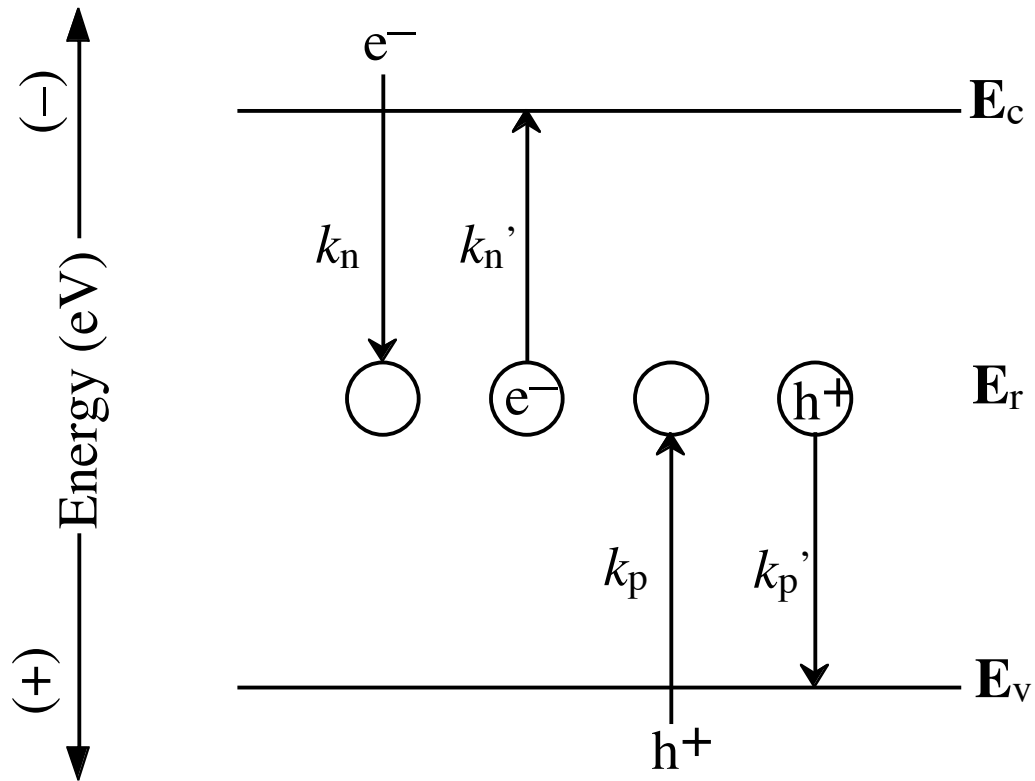
Figure 1.4

A schematic depicting the microscopic balance between electron and hole capture and emission processes at recombination centers in the semiconductor. The k_n and k_p are the capture coefficients of electrons and holes by the recombination centers at an energy level of E_r, respectively. The k_n' and k_p' are the thermal emission coefficients of electrons and holes from the recombination centers back to the conduction and valence bands, respectively. The E_c and E_v are energies of conduction and valence band edges.

4.4.   Depletion-Region Recombination

Depletion-region recombination can also be calculated using SRH statistics. We use the Equation 1.14 derived in the previous section, and drop the subscript "s" in all parameters to yield the following expression, with N_r (having a unit of cm^{-3}) now accounts for the density of recombination centers within the semiconductor:

$$U = N_r \frac{k_n k_p (np - n_i^2)}{k_n(n + n_1) + k_p(p + p_1)} \tag{1.19}$$

Since only those recombination centers with energy levels at the mid-gap are the most effective traps, we can assume $k_n = k_p$. To obtain the depletion-region recombination current, U has to be integrated over the limits of depletion region. The value of U has a large dependence on both n and p, and the maximum value of U exist when $n = p$.

$$U_{max} = \frac{n_i}{2\tau_p} \exp(-qV / 2kT) \tag{1.20}$$

The integral $\int U(x)dx$ can then be replaced by the U_{max} multiplied by a width over which this maximum rate occurs. The effective width for the integration is $kTW/q(V_{bi}+V)$, and the depletion-region recombination current can be obtained:

$$J = \int_0^{kTW/q(V_{bi}+V)} qU dx = \frac{kTWn_i}{2\tau_p(V_{bi} + V)} \exp(-qV / 2kT) \tag{1.21}$$

From equation 1.21, a γ of 2 is often an indication that the recombination current is dominated by the depletion-region recombination. Assuming J_{dr} dominates the recombination current, substituting $n_i = (N_c N_v)^{1/2}\exp(\mathbf{E}_g/2kT)$ into equation 1.19 yields an expression for the J_0:

$$J_0 = \frac{kTW(N_c N_v)^{1/2}}{2\tau_p (V_{bi} + V)} \exp(-\mathbf{E}_g / 2kT) \exp(-qV / 2kT) \qquad (1.22)$$

4.5. Bulk-Region Recombination

The current for the bulk recombination process is a function of hole diffusion rate into the bulk region of the semiconductor. Assuming that depletion-region recombination does not occur, and at any point x, the recombination rate in the bulk is the same as the diffusion rate:

$$[p(x) - p_0(x)] / \tau_p + D_p \frac{\delta^2 p(x)}{\delta x^2} = 0 \qquad (1.23)$$

where $p(x)$ and $p_0(x)$ are the hole concentration and the equilibrium hole concentration at a point x in the bulk, and D_p is the hole diffusion coefficient. Since the total current at steady state is the same everywhere in the bulk, the total bulk recombination current can be determined by solving the hole concentration at the deletion layer edge. Two boundary conditions will be applied. First is the assumption of the absence of depletion-region recombination at the depletion layer edge $x = W$:

$$n(W)p(W) = n_i^2 \exp(-qV / kT) \qquad (1.24)$$

Because the injected minority carrier concentration is much lower than the dopant density, $n(W) \approx n(W)$, and equation 1.24 becomes

$$p(W) = p_0 \exp(-qV / kT) \qquad (1.25)$$

Adding in the second boundary condition that all the holes recombine in the bulk before reaching the ohmic contact, $p(\infty) = p_0$, $p(x)$ can be solved:

$$p(x) = p_0 + p_0[\exp(-qV \,/\, kT) - 1]\exp[-(x - W) \,/\, L_p) \tag{1.26}$$

where L_p is the hole diffusion length. Substituting this expression into $J_p = qD[dp(x)/dx]$, and then the current at $x = W$ can be evaluated:

$$J_p(W) = \frac{qD_p p_0}{L_p}[\exp(-qV \,/\, kT) - 1] \tag{1.27}$$

If the bulk-region recombination is the dominant mechanism, the γ is expected to be 1, and the activation energy $\mathbf{E_g}$. If $J_p(W)$ is equal to the total bulk recombination current:

$$J_0 = \frac{qD_p p_0}{L_p} = \frac{qD_p n_i^2}{L_p N_d} \tag{1.28}$$

5. Surface States[10]

In order to improve the efficiency and the stability of photoelectrochemical or photovoltaic devices, the unfavorable current due to recombination has to be suppressed. While many strategies to improve the solar energy conversion devices have been researched by others, the central theme of this thesis is to approach the challenge by investigating the surface states at the semiconductor/liquid junction and proposing a solution to improve the stability by surface modification. As the size of semiconductor devices continues to decrease, the effects of surface defects also become considerably more significant. Understanding of semiconductor surface properties and developments of methods that can improve the electrical properties of semiconductors can certainly provide unimaginable benefits for technologies of the future.

The different orbital structure of a semiconductor surface compared to its bulk usually results in one or more energy levels located inside of the bandgap region. These localized surface states can be either intrinsic or extrinsic in nature. The intrinsic surface states can arise because the surface atoms of a semiconductor do not have the periodic bonding structure that exists in the crystal lattice, or due to the reconstruction of the surface. The extrinsic surface states are the result of interface formation. Surface defects can emerge if a reaction or bonding occurs between the two phases in contact, and the adsorption or attachment of chemical impurities can also contribute to the surface states.

Although not all surface bonds produce deleterious surface states, those reside in the bandgap can unquestionably affect the electrical properties of a semiconductor. The presence of these surface states can provide recombination centers and reduce the carrier lifetime. They can also serve as sinks or sources for electrical charges, which can have negative effects on the junction potential. As Chapter 2 demonstrates the existence of surface states at n-GaAs/CH_3CN interfaces and how it modifies the junction behavior, the

works presented in Chapters 3 and 4 involve surface modification of Si and the effects on the solid-state junction behaviors. Surface modification can be one of the easiest methods to create stable surface bonds that do not cause the rise of surface states, while also provide a barrier against corrosion or destructive oxidation.

6. References

(1)   Tan, M. X.; Laibinis, P. E.; Nguyen, S. T.; Kesselman, J. M.; Stanton, C. E.; Lewis, N. S. *Prog. Inorg. Chem.* **1994**, *41*, 21.

(2)   Chapin, D. M.; Fuller, C. S.; Pearson, G. L. *J. Appl. Phys.* **1954**, *25*, 676.

(3)   Fahrenbruch, A. L.; Bube, R. H. *Fundamentals of Solar Cells: Photovoltaic Solar Energy Conversion*; Academic: New York, 1983.

(4)   Kumar, A.; Wilisch, W. C. A.; Lewis, N. S. *CRC Critical Rev.* **1993**, *18*, 327.

(5)   Rhoderick, E. H.; Williams, R. H. *Metal-Semiconductor Contacts*; 2nd ed.; Oxford University Press: New York, 1988.

(6)   Sharma, B. L., Ed. *Metal-Semiconductor Schottky Barrier Junctions and Their Applications*; Plenum: New York, 1984.

(7)   Sze, S. M. *The Physics of Semiconductor Devices*; 2nd ed.; Wiley: New York, 1981.

(8)   Weast, R. C.; Astle, M. J.; Bayer, W. H. *Handbook of Chemistry and Physics*; 71st ed.; CRC Press: Boca Baton, FL., 1991.

(9)   Fonash, S. J. *Solar Cell Device Physics*; Academic: New York, 1981.

(10)   Lewis, N. S.; Rosenbluth, M. In *Photocatalysis: Fundamentals and Applications*; Serpone, N., Pelizzetti, E., Eds.; John Wiley & Sons: New York, 1989, pp 45.

(11)   Crowell, C. R.; Sze, S. M. *Solid State Elec.* **1966**, *9*, 1035.

(12)   Memming, R. In *Electroanalytical Chemistry*; Bard, A. J., Ed.; Marcel Dekker, Inc.: New York, 1979; Vol. 11, p 1.

(13)   Gerischer, H. In *Physical Chemistry: An Advanced Treatise*; Eyring, H., Henderson, D., Yost, W., Eds.; Academic: New York, 1970; Vol. 9A, pp 463.

(14)   Shockley, W.; Read, W. T. *Phys. Rev.* **1952**, *87*, 835.

(15)   Hall, R. N. *Phys. Rev.* **1952**, *87*, 387.